

UC Davis

UC Davis Previously Published Works

Title

PLK4 is upregulated in prostate cancer and its inhibition reduces centrosome amplification and causes senescence.

Permalink

<https://escholarship.org/uc/item/2pp799bz>

Journal

The Prostate, 82(9)

Authors

Singh, Chandra

Denu, Ryan

Nihal, Minakshi

et al.

Publication Date

2022-06-01




DOI

10.1002/pros.24342

Peer reviewed

## ORIGINAL ARTICLE

# PLK4 is upregulated in prostate cancer and its inhibition reduces centrosome amplification and causes senescence

Chandra K. Singh PhD<sup>1</sup>  | Ryan A. Denu MD, PhD<sup>2,3,4</sup> | Minakshi Nihal PhD<sup>1</sup> |  
Maria Shabbir PhD<sup>1</sup> | Debra R. Garvey PhD<sup>1</sup> | Wei Huang MD<sup>5</sup> |  
Kenneth A. Iczkowski MD<sup>6</sup>  | Nihal Ahmad PhD<sup>1,4,7</sup> 

<sup>1</sup>Department of Dermatology, School of Medicine and Public Health, University of Wisconsin, Madison, Wisconsin, USA

<sup>2</sup>Medical Scientist Training Program, School of Medicine and Public Health, University of Wisconsin, Madison, Wisconsin, USA

<sup>3</sup>Department of Medicine, Division of Hematology/Oncology, School of Medicine and Public Health, University of Wisconsin, Madison, Wisconsin, USA

<sup>4</sup>Carbone Cancer Center, University of Wisconsin, Madison, Wisconsin, USA

<sup>5</sup>Department of Pathology and Laboratory Medicine, University of Wisconsin, Madison, Wisconsin, USA

<sup>6</sup>Department of Pathology, Medical College of Wisconsin, Milwaukee, Wisconsin, USA

<sup>7</sup>William S. Middleton VA Medical Center, Madison, Wisconsin, USA

## Correspondence

Nihal Ahmad PhD, Department of Dermatology, Wisconsin Institutes for Medical Research, University of Wisconsin, 1111 Highland Ave, Room 7045, Madison, WI 53705, USA.  
Email: [nahmad@dermatology.wisc.edu](mailto:nahmad@dermatology.wisc.edu)

## Present address

Maria Shabbir, Atta-ur-Rahman School of Applied Biosciences, National University of Sciences and Technology, Islamabad, Pakistan.

## Funding information

U.S. Department of Veterans Affairs, Grant/Award Numbers: I01CX001441, 1I01BX004221, 1K6BX003780; National Institutes of Health, Grant/Award Numbers: F30CA203271, T32GM008692, P30 CA014520, S10OD023526, R01CA176748

## Abstract

**Background:** Identification of novel molecular target(s) is important for designing newer mechanistically driven approaches for the treatment of prostate cancer (PCa), which is one of the main causes of morbidity and mortality in men. In this study, we determined the role of polo-like kinase 4 (PLK4), which regulates centriole duplication and centrosome amplification (CA), in PCa.

**Materials and Methods:** Employing human PCa tissue microarrays, we assessed the prevalence of CA, correlated with Gleason score, and estimated major causes of CA in PCa (cell doubling vs. centriole overduplication) by staining for mother/mature centrioles. We also assessed PLK4 expression and correlated it with CA in human PCa tissues and cell lines. Further, we determined the effects of PLK4 inhibition in human PCa cells.

**Results:** Compared to benign prostate, human PCa demonstrated significantly higher CA, which was also positively correlated with the Gleason score. Further, most cases of CA were found to arise by centriole overduplication rather than cell doubling events (e.g., cytokinesis failure) in PCa. In addition, PLK4 was overexpressed in human PCa cell lines and tumors. Moreover, PLK4 inhibitors CFI-400945 and centrinone-B inhibited cell growth, viability, and colony formation of both androgen-responsive and androgen-independent PCa cell lines. PLK4 inhibition also induced cell cycle arrest and senescence in human PCa cells.

Chandra K. Singh and Ryan A. Denu contributed equally to this study.

This is an open access article under the terms of the Creative Commons Attribution-NonCommercial-NoDerivs License, which permits use and distribution in any medium, provided the original work is properly cited, the use is non-commercial and no modifications or adaptations are made.

© 2022 The Authors. *The Prostate* published by Wiley Periodicals LLC

**Conclusions:** CA is prevalent in PCa and arises predominantly by centriole overduplication as opposed to cell doubling events. Loss of centrioles is cellular stress that can promote senescence and suggests that PLK4 inhibition may be a viable therapeutic strategy in PCa.

**KEYWORDS**

centriole overduplication, centrosome, CFI-400945, PLK4, prostate cancer

## 1 | INTRODUCTION

The serine/threonine kinase, polo-like kinase 4 (PLK4) is required for centriole duplication. Abnormal centriole duplication can disrupt the normal choreography of cell division, leading to chromosomal instability and tumorigenesis. Centrosome amplification (CA) is one mechanism leading to chromosomal instability in cancer and is generally associated with higher risk subtypes of cancers and worse patient outcomes.<sup>1</sup> Prostate cancer (PCa), the most commonly diagnosed noncutaneous cancer in men<sup>2</sup> has been associated with cell division errors leading to chromosomal instability. CA has previously been reported in PCa,<sup>3–5</sup> and it appears to be an early event, as it is found in prostatic intraepithelial neoplasia,<sup>6</sup> a precursor to PCa. Specifically, centrosome size and number, as well as pericentrin (a component of pericentriolar material (PCM)) levels, are greater in tumors with higher grades and Gleason scores.<sup>4–6</sup> Moreover, CA correlates with aneuploidy in PCa.<sup>5</sup> The underlying causes of CA in PCa are not clear. The two major causes of CA are believed to be (i) cell doubling events (cytokinesis failure or cell fusion) and (ii) centriole overduplication.<sup>7</sup> In melanoma, centriole overduplication has been found to be the predominant mechanism of CA.<sup>8</sup> However, the mechanism of CA in several other cancers, including PCa is not clearly understood.

It is well known that PLK4 localizes to centrioles and coordinates duplication of centrioles in the late G1 and early S phases of the cell cycle.<sup>9,10</sup> Increased PLK4 expression has been associated with poor outcomes in several human cancers, including colorectal,<sup>11</sup> breast,<sup>12,13</sup> melanoma,<sup>8</sup> and neuroblastoma.<sup>14</sup> Proper control of PLK4 expression and activity are crucial, as *Plk4*<sup>+/-</sup> mice are predisposed to hepatocellular carcinoma,<sup>15</sup> while overexpression causes CA, induces tumorigenesis,<sup>16,17</sup> and promotes invasion and metastasis.<sup>18–21</sup> The role of PLK4 in PCa has not been well studied. One clue of the involvement of PLK4 in PCa comes from the finding that *CAND1* is upregulated in PCa and promotes CA by enhancing PLK4 stability.<sup>22</sup> Another clue of PLK4 involvement in PCa comes from a recently published study where hypoxia-inducible factor-1 $\alpha$  (HIF1 $\alpha$ ) has been demonstrated to induce CA by upregulating PLK4 in multiple cancers including PCa.<sup>23</sup>

Herein, we evaluated the cause of CA in PCa, determined the role of PLK4 in CA in PCa, analyzed the prognostic value of PLK4 expression in PCa, and explored the potential of PLK4 inhibition as a strategy to treat PCa.

## 2 | MATERIALS AND METHODS

### 2.1 | Tissue microarray (TMA), immunofluorescence (IF), and immunohistochemistry (IHC)

IF staining for analysis of centrosomes was performed with a human prostate TMA (US Biomax #PR8011a; Table S1A) containing cases of 32 prostatic adenocarcinomas, 2 metastases, 26 prostatic hyperplasia, 6 chronic inflammation, 6 normal adjacent, and 8 normal prostate samples. IF staining followed by imaging was carried out as previously described<sup>1,8</sup> using anti-pericentrin (Abcam, ab4448, 1:200), anti-CEP164 (a kind gift from Dr. Erich Nigg, 1:100),<sup>24</sup> and anti-pan-cytokeratin (Abcam, ab7753, 1:200) primary antibodies and Alexa Fluor-conjugated secondary antibodies (Jackson ImmunoResearch Laboratories). Scoring of centrosomes was performed using Nikon Eclipse Ti inverted microscope using  $\times 100$  objective and CoolSNAP HQ2 charge-coupled device camera (Photometrics). Centrosomes were analyzed from at least three different regions of tumor core. The number of pericentrin foci, as well as foci that overlapped with CEP164, were quantified in cells expressing cytokeratins, an epithelial marker. Cytokeratin staining also allowed for the delineation of individual cells. For representative images, Z stacks were acquired at a step size of 0.2  $\mu\text{m}$  and deconvolved using Nikon Elements.

IHC for PLK4 analysis was performed with another human prostate TMA (US Biomax #PR956; 40 cases/95 cores; Table S1B) containing 40 cancer and 8 matched normal adjacent tissues. The TMA was immunostained with PLK4 antibody (Abcam, ab137398, 1:200) using Vector Red Alkaline Phosphatase substrate and Vectastain ABC-AP Kit (Vector Labs), as described previously.<sup>25</sup> Hematoxylin was used to counterstain nuclei. The PLK4 antibody used in this study was previously validated by observing PLK4 localization to the centrosome in PLK4-overexpressing RPE-1 cells.<sup>8</sup> The stained TMA was scanned using Vectra System (PerkinElmer) and analyzed using inForm Software. An 8-bit image cube from each of the tissue cores was acquired to segment tissues (epithelium vs. stroma) and cells (nucleus vs. cytoplasm) to analyze PLK4 protein levels. PLK4 staining indicated by the intensity of red color from Vector Red chromogen was quantitated within tissues and subcellular compartment(s) after unmixing signals with inForm software.

## 2.2 | Cell culture and immunofluorescence

Human PCa cell lines 22Rv1, DU145, PC3, LNCaP, and C4-2 (ATCC) were grown in RPMI1640 media with 10% fetal bovine serum under standard culture conditions. The cell lines were authenticated by STR analysis using Promega PowerPlex 16HS System Kit (DC2101) at the University of Wisconsin Translational Research Initiatives in Pathology) laboratory. These cells were also routinely tested for mycoplasma using Mycoplasma Plus Detection Kit (Lonza) according to the manufacturer's protocol. Human primary prostate epithelial cells (HPrEC; ATCC) were grown in prostate epithelial cell basal medium supplemented with multiple growth components (L-glutamine, extract-P, epinephrine, tumor growth factor- $\alpha$  (TGF- $\alpha$ ), hydrocortisone hemisuccinate, insulin, and apo-transferrin). For treatment, PLK4 inhibitors CFI-400945 (Cayman Chemical) and centrinone-B (Med Chem Express) were diluted to 10  $\mu$ M in dimethyl sulfoxide. PCa cells were grown to ~50% confluency and then treated with either CFI-400945 (0, 25, 50, and 100 nM) for 48 or 72 h, or with centrinone-B (0, 50, 100, and 200 nM) for 48 h.

Immunofluorescence analysis with all prostate cell lines was carried out as previously described.<sup>1,8</sup> Antibodies utilized for immunofluorescence include:  $\alpha$ -tubulin (12G10, deposited to DSHB by J. Frankel/E. M. Nelsen; 1:1000), pericentrin (Abcam, ab4448, 1:1000), centrin (Millipore, 04-1624, 1:500),  $\gamma$ -tubulin (Abcam, ab27074, 1:1000) and Alexa Fluor-conjugated secondary antibodies (Invitrogen, 1:350). Cells were counterstained with 4',6-diamidino-2-phenylindole and mounted on glass slides with Prolong Gold antifade medium (Invitrogen).

## 2.3 | Reverse transcription-quantitative real-time PCR (RT-qPCR)

Total RNA was isolated from cells using RNeasy Mini Kit (Qiagen), and complementary DNA was synthesized using oligo(dT) primers, dNTPs, and M-MLV reverse transcriptase (Promega). RT-qPCR was performed using SYBR Premix Ex Taq II (TaKaRa) and appropriate primer sets. PLK4 primers were procured from Sigma. P21 and GAPDH primers were retrieved from Primer Bank.<sup>26</sup> Primer sequences are detailed in Table S2. Relative target messenger RNA (mRNA) levels were calculated by  $\Delta\Delta$ CT comparative method using GAPDH as an endogenous control.

## 2.4 | Immunoblotting

Protein isolation, quantification, and immunoblotting were done as previously reported,<sup>27</sup> PLK4 (Abcam, ab137398, 1:500), P21 (Proteintech, 12952-1-AP, 1:500), and GAPDH (Proteintech, 12952-1-AP, 1:5000) immunoblots were detected using SuperSignal West Femto Chemiluminescent Substrates (Thermo Fisher Scientific) by LI-COR Odyssey Fc Imager.

## 2.5 | Cell proliferation, colony formation, cell cycle, and senescence assays

CFI-400945- and centrinone-B-treated cells were harvested and counted using Trypan Blue dye on the Bio-Rad cell counter. The number of total cells was plotted as percent cell growth, and the number of viable cells in particular samples was plotted as percent cell viability. For colony formation assay,<sup>28</sup> equal numbers (500) of CFI-400945- and centrinone-B-treated viable cells were seeded in 6-well plates and allowed to grow for 2 weeks in a drug-free medium. Colonies were fixed and stained in 1% crystal violet in 2:1:2 acetic acid:methanol:dH<sub>2</sub>O. Plates were scanned and analyzed for colony formation.

For cell cycle analysis, PCa cells were synchronized in serum-free medium for 24 h before treatment with CFI-400945 (0, 25, 50, and 100 nM) for 48 h. Treated cells were collected, washed, and fixed in 70% ethanol overnight. Afterward, RNA was removed with RNase A treatment (Sigma-Aldrich) at 37°C for 30 min and then cells were resuspended in 0.5 ml of phosphate-buffered saline and stained with 50  $\mu$ g/ml propidium iodide (Sigma-Aldrich) and subjected to Attune flow cytometer (Thermo Fisher Scientific) and analyzed with Modfit software.

For senescence analysis, CFI-400945-treated PCa cells were stained using Senescence  $\beta$ -Galactosidase Staining Kit (Cell Signaling) as per the manufacturer's instructions. Senescence-associated  $\beta$ -galactosidase (SA- $\beta$ -gal)-positive cells were imaged and quantified with EVOS XL Core Imaging System.

## 2.6 | Statistical analysis

Analysis of variance and *t* tests were used for the statistical analysis of our data. When multiple means were compared, Tukey's correction or Dunnett multiple comparisons tests were utilized. Correlations were assessed with Pearson's correlation. Two-sided, unpaired statistical tests were used throughout.  $p < 0.05$  was considered statistically significant.

# 3 | RESULTS

## 3.1 | CA is prevalent in human PCa

We analyzed CA in 34 PCa, 26 prostatic hyperplasia, and 20 benign prostate samples by staining a prostate TMA for pericentrin, a component of PCM (Figure 1A). Clinical pathological characteristics of patient samples included in this TMA are detailed in Table S1A. PCa samples demonstrate significantly greater CA compared to prostatic hyperplasia and benign prostate (mean centrosome number is 2.06 for PCa vs. 1.67 for hyperplasia vs. 1.17 for normal; mean percentage of cells with >2 centrosomes is 26.2% for PCa vs. 21.8% for hyperplasia vs. 12.8% for normal; Figures 1B,C and S1A). CA is also significantly greater

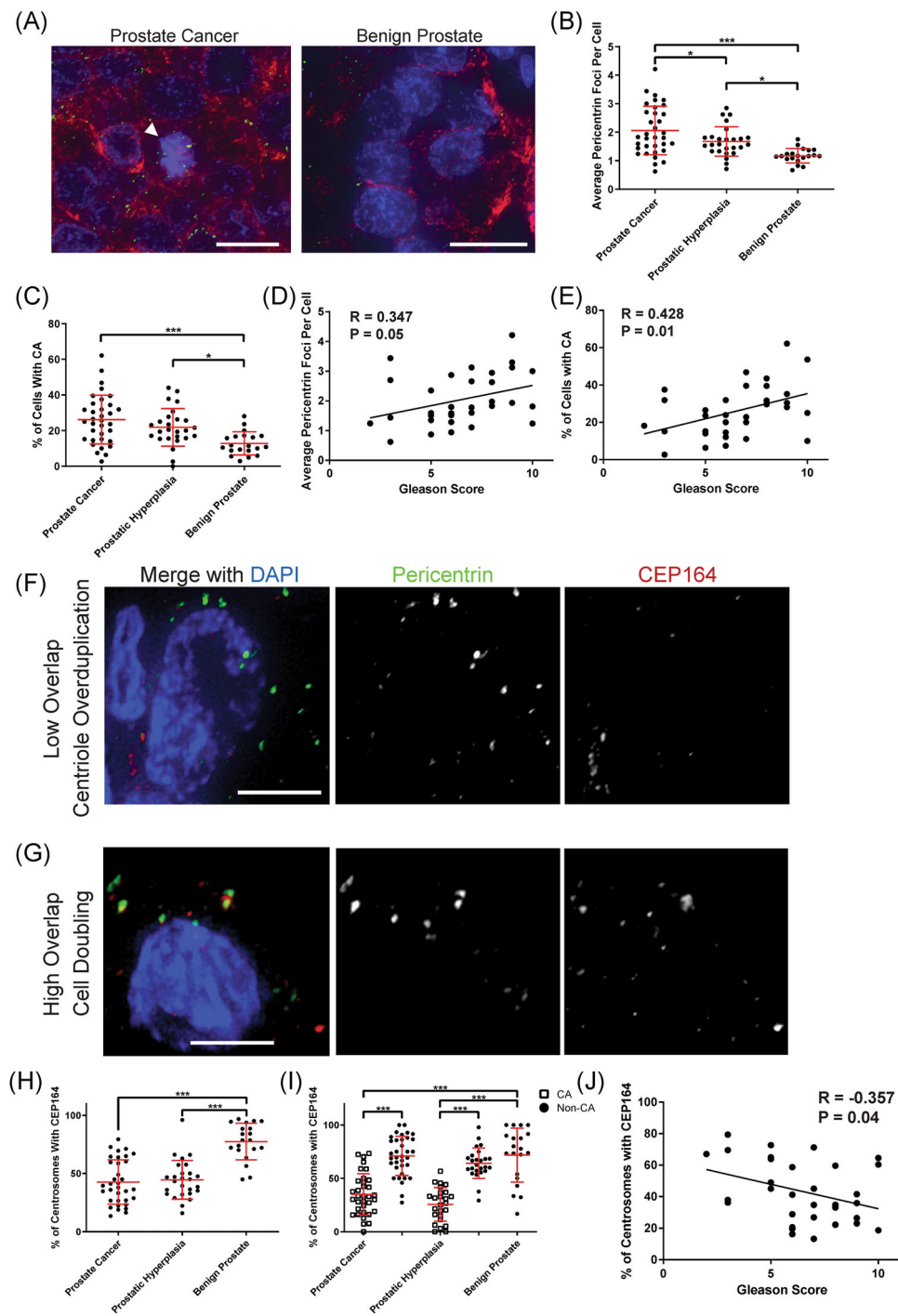


**FIGURE 1** (See caption on next page)

in hyperplastic compared to benign samples. Furthermore, we assessed the clinical significance of CA in this cohort of PCA patients by correlating CA with the Gleason score. Significant, positive correlations are identified between Gleason score and either centrosome number (Figure 1D) or percent of cells with >2 centrosomes (Figure 1E). Overall, our data show that CA is common in PCA and correlates with a high Gleason score.

### 3.2 | CA is predominantly caused by centriole overduplication in PCA

CA can arise by centriole overduplication or cell doubling events (e.g., cytokinesis failure, cell-cell fusion). To estimate the relative contributions of these two mechanisms, we stained a prostate TMA for a marker of mother/mature centrioles, CEP164, which gets

recruited to the centrosome in late G2 or early M phases.<sup>24</sup> If centriole overduplication was present, then we would expect most centrosomes to lack CEP164 staining (Figure 1F). In contrast, if cell doubling was the predominant mechanism of CA, we would expect most centrosomes to contain CEP164 because all these cells would have progressed through G2 before failing cytokinesis (Figure 1G). We empirically validated this assumption by staining for CEP164 in cells overexpressing PLK4 (to model centriole overduplication) and cells in which cytokinesis failure was chemically induced (to model cell doubling). Indeed, cells overexpressing PLK4 demonstrate a lower percentage of centrosomes with CEP164, while cells induced to fail cytokinesis display a higher percentage of centrosomes with CEP164 (Figure S2A,B) as also shown by others.<sup>8,24,29–31</sup> PCa samples display significantly lower percentages of centrosomes with CEP164 (42.6% for PCa vs. 44.5% for hyperplasia vs. 77.4% for normal; Figures 1H and S1B). Furthermore, if we just consider cells with >2 centrosomes (i.e., centrosome-amplified cells), we similarly see significantly lower percentages of centrosomes costaining for CEP164 in PCa and hyperplasia samples compared to cells with 2 or less centrosomes in PCa, hyperplasia, and benign samples (Figure 1I). In addition, we found a significant negative correlation between tumor's percentage of centrosomes with CEP164 and tumor's Gleason score (Figure 1J). Based on our data, we conclude that most cases of CA arise by centriole overduplication rather than cell doubling events.

### 3.3 | PLK4 is overexpressed in human PCa and is required for centriole overduplication

To understand the role of PLK4 and centriole overduplication in PCa, we assessed PLK4 expression in human PCa tissues ( $n = 40$ ) using a TMA with matched normal adjacent tissue ( $n = 8$ ). Compared to benign, we found significantly higher expression of PLK4 in PCa tissues (Figures 2A,B and S3A). Interestingly, there was a trend

toward higher PLK4 with a higher Gleason score in PCa epithelial cells, specifically in cancers with a Gleason score of 10 (Figure 2C). Clinical pathological characteristics of patient samples included in this TMA are detailed in Table S1B. PLK4 staining in an additional TMA containing 25 PCa tissue and 25 benign (matched adjacent prostate) tissues<sup>32</sup> demonstrated higher levels of PLK4 in PCa samples (Figure S3B,C), further confirming that PLK4 is overexpressed in PCa.

Next, we utilized prostate data set from The Cancer Genome Atlas via cBioPortal<sup>34</sup> to assess PLK4 gene expression. Patients with higher PLK4 expression had higher Gleason scores and worse disease-free survival (Figure 2D–F). We also calculated CA20, which represents a score calculated mRNA expression values of certain genes including PLK4 required for centriole duplication.<sup>33</sup> Higher CA20 scores were associated with higher Gleason scores and worse disease-free survival (Figure 2G–I).

### 3.4 | PLK4 is overexpressed in PCa cell lines and its inhibition reduces CA

We assessed the expression profile of PLK4 in multiple PCa cell lines with varied genetic makeup (DU145, 22Rv1, PC3, LNCaP, C4-2) along with normal HPrEC using immunoblot and RT-qPCR analyses. Compared to normal HPrEC, all PCa cell lines showed markedly higher levels of PLK4 protein and mRNA (Figure 3A–C). Next, PCa and HPrEC cells were stained for a centriole marker, centrin, and a component of PCM, pericentrin, to assess centrioles and centrosomes and calculate the percentage of cells with CA (defined as >4 centrin foci, which is the gold standard for assessing CA). Except for LNCaP, all PCa cell lines demonstrated a markedly higher number of centrioles per cell and a higher percentage of cells possessing >4 centrin foci (Figure 3D–E). We also assessed the correlation of PLK4 protein and mRNA levels with average centrioles per cell in each cell line; however, the data remain inconclusive due to the small sample size

**FIGURE 1** Centrosome amplification occurs in PCa, correlates with a higher Gleason score, and arises predominantly by centriole overduplication. (A) Micrographs of centrosomes (pericentrin, green) in PCa (left) and benign prostate specimen (right). Tissues were also stained for cytokeratins (red) and DNA (blue). The white arrowhead denotes a mitotic cell in the middle of PCa image. Scale bars = 10  $\mu$ m. (B) The average centrosome number (assessed by pericentrin foci) in each tumor and benign sample is plotted. Individual cell data for each specimen are shown in Figure S1A. (C) CA was defined as >2 pericentrin foci in a cell. At least 50 cells were assessed in each tumor. Each dot represents one PCa or benign specimen. (D) Correlation of average pericentrin foci per cell versus Gleason score. (E) Correlation of the percent of cells with >2 pericentrin foci versus Gleason score. (F, G) Micrographs of pericentrin (green) and CEP164 (red) staining in PCa demonstrating either low overlap (F) or high overlap (G) of pericentrin and CEP164, suggesting CA via centriole overduplication or cell doubling, respectively. Pericentrin = green, CEP164 = red, and DNA/DAPI = blue. Scale bars = 5  $\mu$ m. (H) A dot-plot comparing the percent of centrosomes (defined by pericentrin staining) that costained for a mother/mature centriole marker (CEP164). Each dot represents the average of cells within one tumor/sample. (I) The cells within each PCa and hyperplastic specimen with >2 pericentrin foci (CA) were further analyzed to determine the cause of CA in these cells. The dot-plot shows the percent of pericentrin foci in these cells that costained with CEP164 (black-outlined squares). For comparison, the percent of pericentrin foci costaining for CEP164 is also shown for cells with 1–2 pericentrin foci in PCa and hyperplastic specimens (black-filled circles). Only non-CA cells are shown for benign specimens, as the number of cells with CA is very low. Each point represents the average of each specimen. Individual cell data for each specimen are shown in Figure S1B. (J) The percent of centrosomes costaining for CEP164 was plotted against tumor's Gleason score. In all panels, bars represent means  $\pm$  SD. \* $p < 0.05$  and \*\*\* $p < 0.001$ . CA, centrosome amplification; DAPI, 4',6'-diamidino-2-phenylindole; PCa, prostate cancer. [Color figure can be viewed at [wileyonlinelibrary.com](http://wileyonlinelibrary.com)]



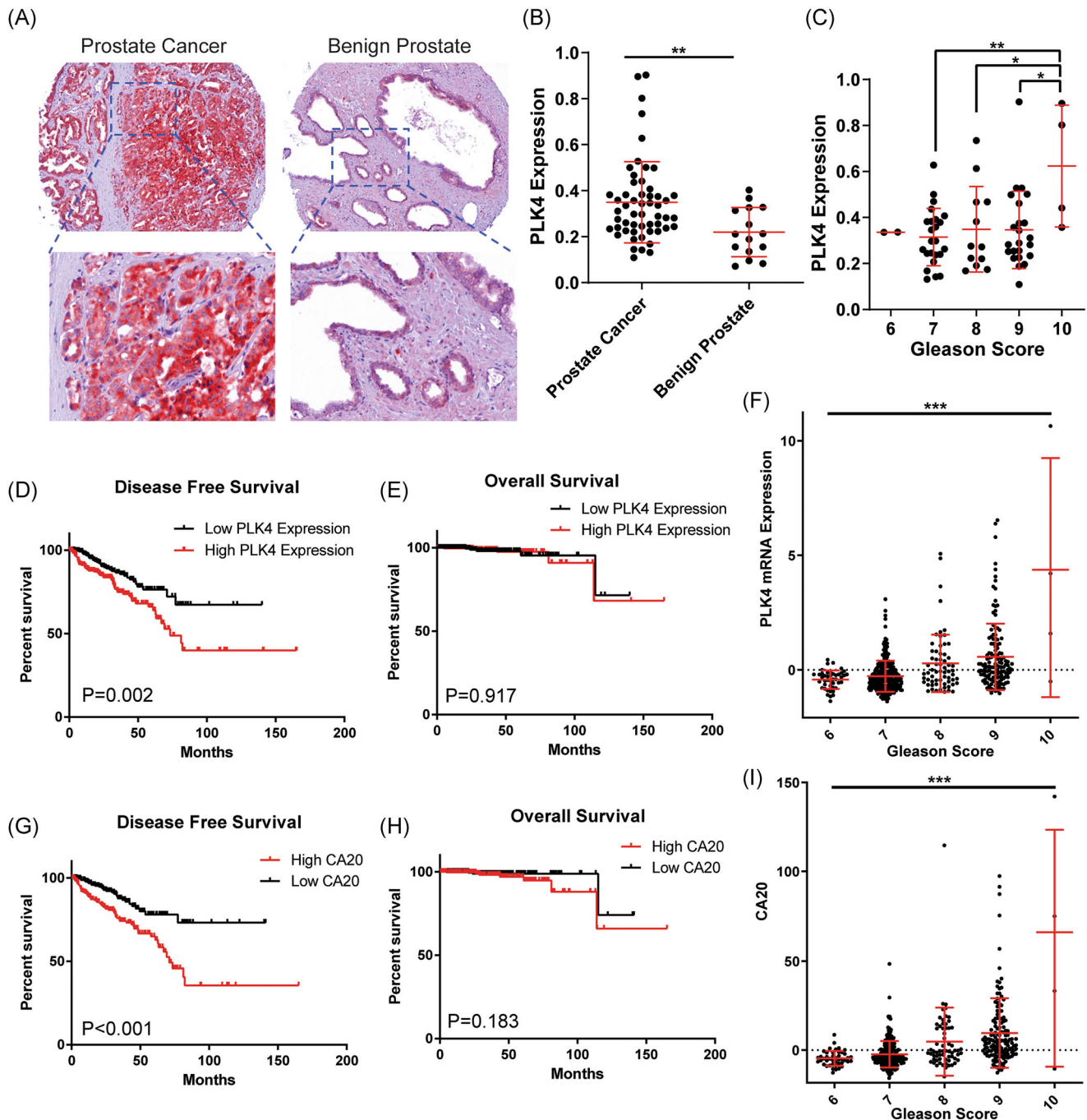


**FIGURE 2** PLK4 is overexpressed in human PCa and its overexpression correlates with worse survival. (A) The representative micrographs of PCa and benign prostate specimen showing PLK4 immunostaining. TMA #PR956 (US Biomax) was immunostained using PLK4 antibody and ABC-alkaline phosphatase reagent followed by incubation with Vector Red chromogen and then hematoxylin as a nuclear counterstain. Images were taken at  $\times 20$  magnification. Dotted areas were zoomed-in using Nuance software. (B) The PLK4-stained slide was scanned using Vectra system and analyzed using the inForm software for PLK4 optical density (OD) as a measure of the stain in each tissue core. The graph was plotted and *t* tests was used for statistical comparison. (C) PLK4 level was also plotted as per Gleason grade in PCa. Next, (D) disease-free survival (DFS) and (E) overall survival (OS) were analyzed based on PLK4 mRNA expression from the 497 PCa patients with available survival data from TCGA; cBioPortal (33) was used to query the data. PLK4 mRNA Z score of 0 was used as a cutoff for “low” versus “high” PLK4 expression. (F) PLK4 expression levels based on Gleason score. (G,H) CA20 was calculated as described by Ogden et al.<sup>33</sup> CA20 incorporates PLK4 along with *AURKA*, *CCNA2*, *CCND1*, *CCNE2*, *CDK1*, *CEP63*, *CEP152*, *E2F1*, *E2F2*, *LMO4*, *MDM2*, *MYCN*, *NDRG1*, *NEK2*, *PIN1*, *PLK1*, *SASS6*, *STIL*, and *TUBG1* genes. Patients were stratified into two groups using the median CA20 score. The Kaplan–Meier method was employed to plot the survival curves, and *p* values shown on the survival curves were determined by log-rank tests. (I) CA20 scores based on Gleason score. ANOVA was used for statistical comparisons of groups in panels (C,F, and I), and bars represent means  $\pm$  SD. \**p* < 0.05; \*\**p* < 0.01, and \*\*\**p* < 0.001. ABC, avidin/biotin complex; ANOVA, analysis of variance; CA20, centrosome amplification 20; mRNA, messenger RNA; PCa, prostate cancer; PLK4, polo-like kinase 4; TMA, tissue microarray. [Color figure can be viewed at [wileyonlinelibrary.com](http://wileyonlinelibrary.com)]

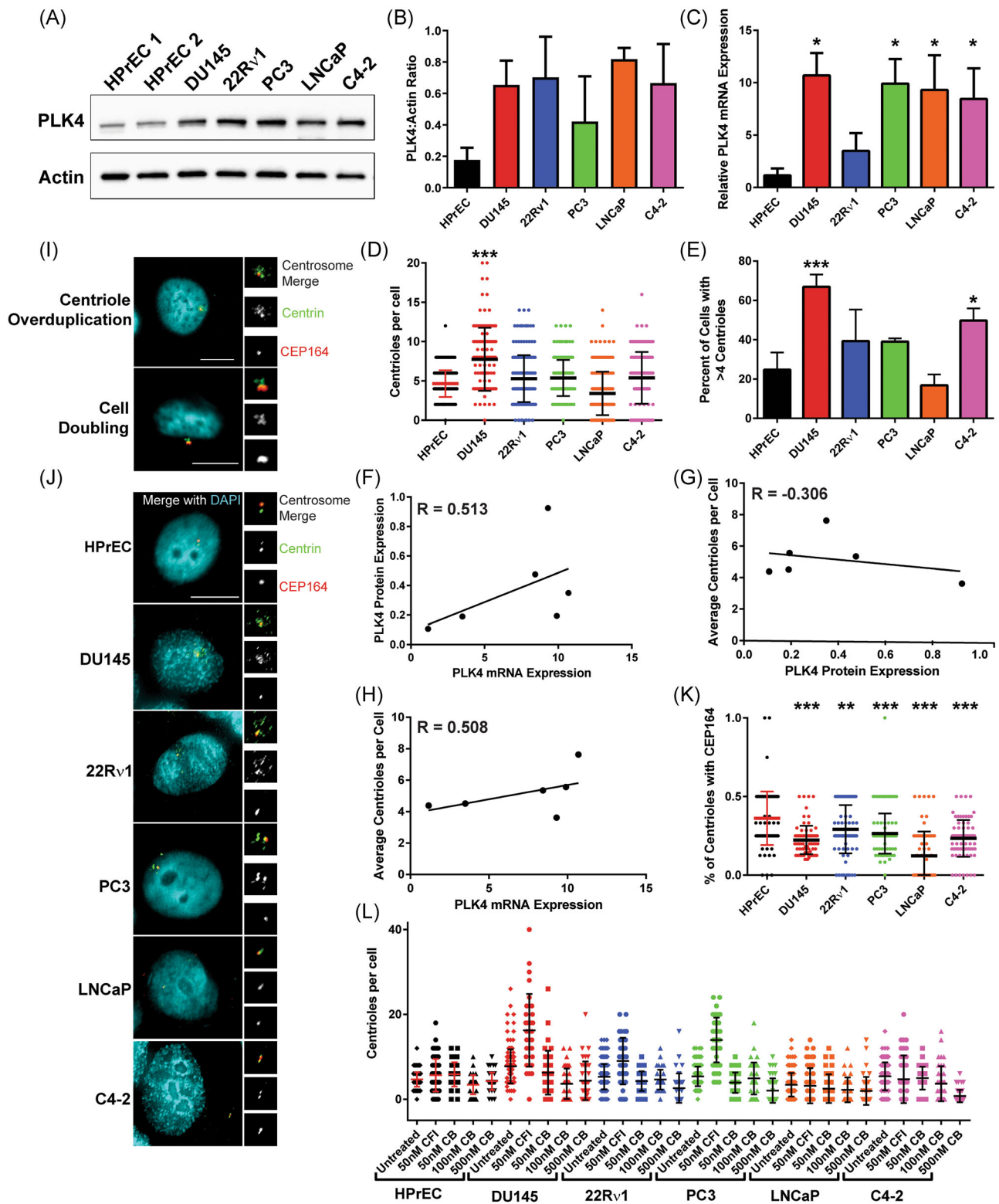


**FIGURE 3** (See caption on next page)

(Figure 3F–H). Further, we determined whether CA in PCa was due to centriole overduplication (low percentage of centrosomes with mother centrioles) or cell doubling (high percentage of centrosomes with mother centrioles) in our selected PCa cell lines

(Figure 3I). We found significantly decreased percentages of centrioles with CEP164 in PCa cell lines compared to normal HP rEC, suggesting that centriole overduplication is more prevalent than cell doubling (Figure 3J–K). Subsequently, centrioles



were analyzed in response to PLK4 inhibition by two different chemical inhibitors of PLK4, CFI-400945 and centrione-B, in PCa cells. Treatment with CFI-400945 increased CA in DU145, 22Rv1 and PC3 cells, and no change was seen in LNCaP and C4-2

cells. However, treatment with centrione-B (500 nM) markedly depleted centrioles in all PCa cells tested (Figure 3L). CFI-400945 and centrione-B specificity and sensitivity differ, and thus it may have caused different effects on centrioles.

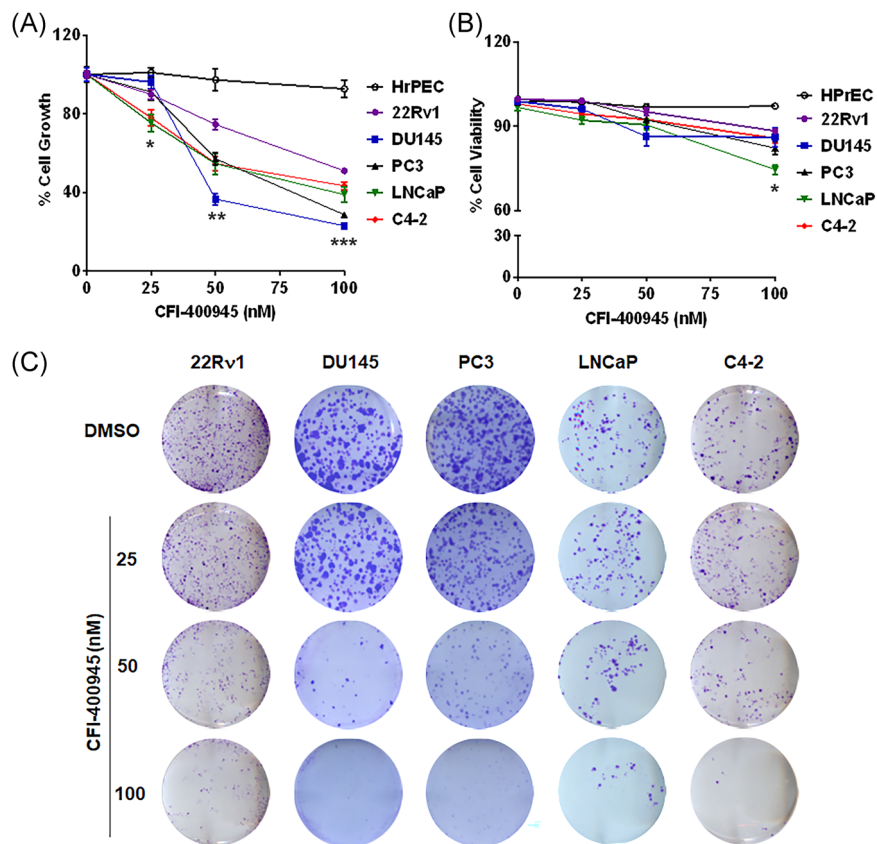


**FIGURE 4** PLK4 inhibition with small-molecule inhibitor CFI-400945 significantly reduces cell growth, viability and colony formation of human PCa cells. (A,B) PCa cells were treated at specified concentrations of CFI-400945 (0, 25, 50, 100 nM) for 72 h, followed by cell growth and viability analyses using Trypan blue exclusion assay. The data were analyzed with GraphPad Prism 5 software using one-way ANOVA followed by Dunnett's multiple comparison tests. The data are presented as means  $\pm$  SEM with statistical significance ( $*p < 0.05$ ;  $**p < 0.01$ , and  $***p < 0.001$ ). The statistical significance represents for all the PCa cell lines compared to HrPEC at specified CFI-400945 concentrations (except for DU145 cell growth at 25 nM, which is not significant). (C) For colony formation analysis, PCa cells were treated for 72 h with CFI-400945 at specified concentrations. These treated cells were then harvested and replated equally (500 cells) in six-well plates and allowed to grow for approximately 2 weeks. Colonies were stained with 1% crystal violet, washed, and air-dried followed by digital photography. CA, centrosome amplification; DMSO, dimethyl sulfoxide; PCa, prostate cancer; PLK4, polo-like kinase 4. [Color figure can be viewed at [wileyonlinelibrary.com](http://wileyonlinelibrary.com)]

**FIGURE 3** PLK4 overexpression correlates with CA in PCa cell lines and is reversed by PLK4 inhibition. (A) Immunoblotting for PLK4 and actin in PCa cell lines (DU145, 22Rv1, PC3, LNCaP, and C4-2) compared to normal prostate epithelial cells (HPrEC) (B) Quantification of protein bands (ratio of PLK4:actin) from immunoblotting. Bars represent means  $\pm$  SD from three blots. (C) RT-qPCR analysis of PLK4 in PCa cell lines compared to HPrEC. GAPDH was used as an endogenous control. (D) Quantification of centrioles in each of prostate cell lines. (E) The percentage of cells with CA (defined as  $>4$  centriole foci) is plotted for each cell line. (F) Correlation of PLK4 protein and mRNA levels in prostate cell lines. (G) Correlation of centrioles with PLK4 protein expression from immunoblotting. (H) Correlation of centrioles with PLK4 mRNA. (I) Examples of HPrEC cells exhibiting centriole overduplication (low percentage of centrosomes with mother centrioles; induced by PLK4 overexpression) and cell doubling (high percentage of centrosomes with mother centrioles; induced by cytochalasin D). Scale bar = 10  $\mu$ m. (J) Representative images of prostate cell lines stained with centrin and CEP164. Scale bar = 10  $\mu$ m. (K) Quantification of the percentage of centrioles with CEP164. Each dot represents one cell. (L) Number of centrioles in each cell line treated with CFI-400945 (50 nM for 48 h) or centrione-B (50, 100, or 500 nM for 48 h). Each dot represents a single cell. Bars represent means  $\pm$  SD and statistical significance is indicated as  $*p < 0.05$ ;  $**p < 0.01$ , and  $***p < 0.001$ . CA, centrosome amplification; HPrEC, human primary prostate epithelial cell; PCa, prostate cancer; PLK4, polo-like kinase 4; RT-qPCR, reverse transcription-quantitative real-time PCR. [Color figure can be viewed at [wileyonlinelibrary.com](http://wileyonlinelibrary.com)]

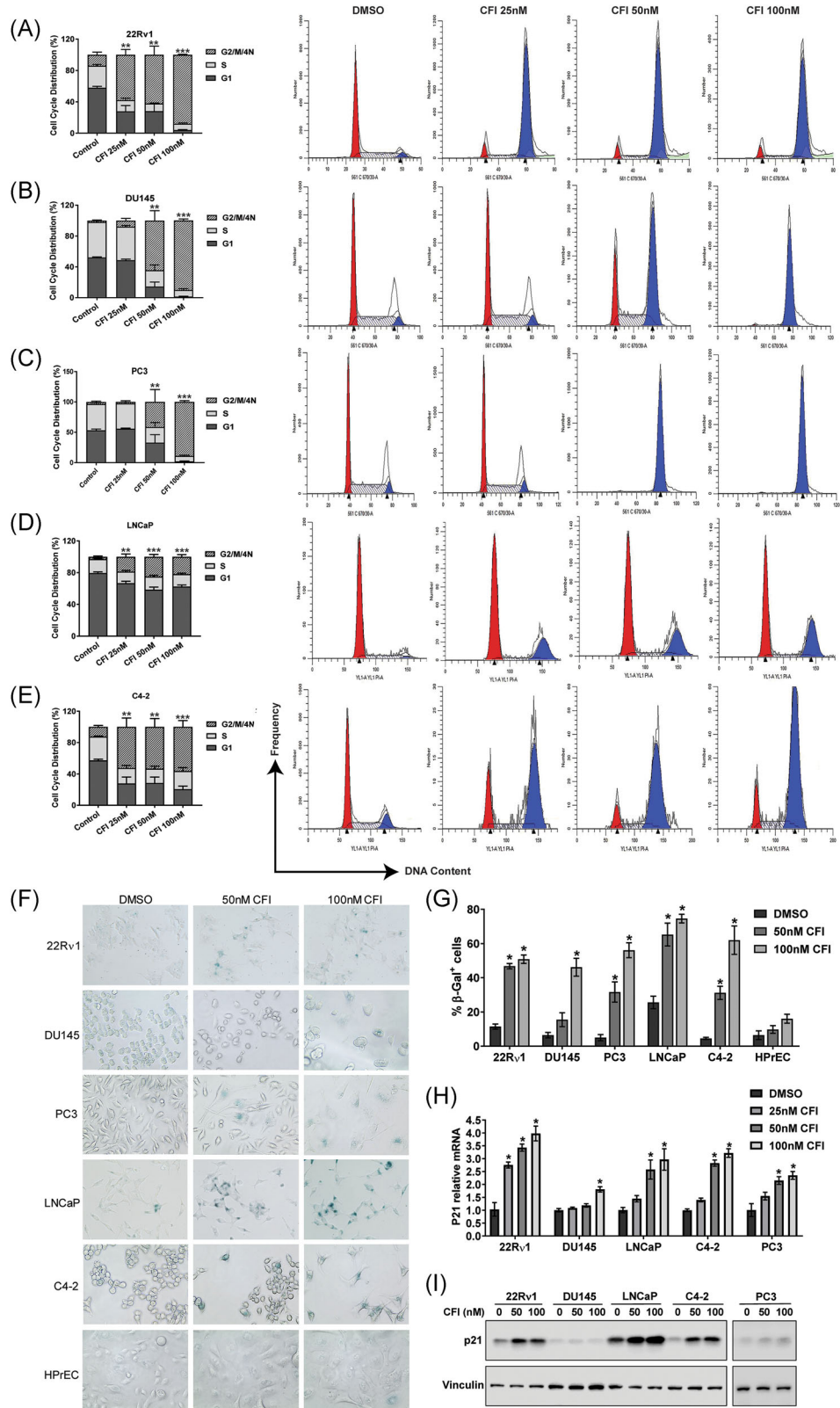


FIGURE 5 (See caption on next page)

### 3.5 | PLK4 inhibition decreases proliferation, viability, and colony formation of PCa cells

To explore the therapeutic potential of PLK4 inhibitors in PCa, we determined the effects of CFI-400945, an orally available PLK4 inhibitor<sup>35,36</sup> on androgen-responsive human PCa cells (22Rv1, LNCaP) and androgen-independent PCa cells (DU145, PC3, C4-2). PCa cell lines treated with CFI-400945 exhibited enlarged and irregular shapes (Figure S4), and CFI-400945 treatment resulted in a significant decrease in cell growth at all three doses for all the PCa cell lines tested, except DU145 at 25 nM (Figure 4A). The cell viability was relatively less affected, and a significant reduction in viability was only seen at 100 nM CFI-400945 (Figure 4B). Notably, cell growth and viability for HPrEC were almost unaffected by CFI-400945 at the concentrations selected in our study (Figure 4A,B). Subsequently, we assessed the effect of PLK4 inhibition on long-term colony formation of human PCa cell lines where CFI-400945-treated cells were allowed to grow for 2 weeks in a drug-free medium. PLK4 inhibition resulted in a marked inhibition of colony formation in PCa cells (Figure 4C). Next, the effect of another PLK4 inhibitor, centrinone-B,<sup>37</sup> was also tested against PCa cells. Concordantly, centrinone-B significantly reduces cell viability and colony formation in PCa cell lines (Figure S5A–C).

### 3.6 | PLK4 inhibition induces cell cycle arrest in the G2/M phase and senescence-like phenotypes in human PCa cells

Given the aforementioned finding that CFI-400945 had a stronger effect on cell growth compared to cell viability, we assessed whether CFI-400945 causes cell cycle arrest. We found that CFI-400945 treatment results in dose-dependent G2/M phase cell cycle arrest in DU145, 22Rv1, PC3, LNCaP, and C4-2 cells (Figure 5A–E). The G2/M arrest was accompanied by a reduction in the G1 and S phases of the cell cycle. The finding of increased G2/M arrest, paired with the observation of reduced colony formation, suggests the possibility of induction of senescence in these CFI-400945-treated PCa cells. To assess this, we determined the effect of CFI-400945 treatment on SA- $\beta$ -Gal in PCa cells. CFI-400945 treatment significantly increased SA- $\beta$ -Gal-positive cells in all five PCa cell lines tested (Figure 5F–G).

The effect on HPrEC cells was less pronounced. We also assessed the effect of CFI-400945 treatment on senescence-associated marker CDKN1A (p21) and found a dose-dependent increase in CDKN1A mRNA and protein levels in all five PCa cell lines tested (Figure 5H,I). We conclude that CFI-400945 causes senescence in PCa cell lines.

## 4 | DISCUSSION

PLK4 has been gaining attention as a potential therapeutic target for cancer treatment. Our data demonstrate that PLK4 is upregulated in human PCa, which is consistent with the reported proproliferative role of PLK4 in other cancers.<sup>8,11–14</sup> Our data demonstrate reduced cellular growth, viability, and colony formation of human PCa cells upon treatment with PLK4 inhibitors. Furthermore, PLK4 inhibition was found to induce senescence in PCa cells. We observed an increase in either tetraploid or G2/M cells after CFI-400945 treatment. There are several explanations for this observation. One possibility is that PLK4 may function at the G2/M transition. Concordantly, PLK4 expression is known to be low during the G1 phase, relatively high during the S phase, and reaches its apex during the G2/M phase.<sup>38</sup> Also, fibroblasts from individuals with Seckel syndrome caused by homozygous loss-of-function mutations in PLK4 show G2/M delay.<sup>39</sup> Alternatively, it is possible that these PLK4 inhibitors caused cytokinesis failure, although cytokinesis failure is not commonly seen with loss of PLK4 or centrioles,<sup>40,41</sup> making this explanation less likely. Lastly, it is possible that these compounds may have off-target effects that explain this; for example, CFI-400945 also inhibits Aurora B (albeit at higher concentration), which can result in cytokinesis failure.<sup>35,37</sup> Coupled with our finding that CFI-400945 increases CA, it is, therefore, most likely that the increase in 4N cells is due to off-target inhibition of Aurora B and subsequent cytokinesis failure.

Prior studies have linked centrosome dysfunction with senescence. It has been shown that a loss of centrioles by PLK4 inhibition induces cell cycle arrest and senescence.<sup>42</sup> Cell cycle arrest following a loss of centrioles is mediated by p53, p53-binding protein 53BP1, deubiquitinase USP28, and ubiquitin ligase TRIM37.<sup>43–45</sup> The promotion of senescence has been a desirable trait in developing anticancer agents. Senescence can exhibit dichotomous tumorigenic properties. Senescence can be triggered by many different stimuli,

**FIGURE 5** PLK4 inhibition by CFI-400945 induces cell cycle arrest in the G2/M phase and senescence-like phenotypes in human PCa cells. (A–E) PCa cell lines DU145, 22Rv1, PC3, LNCaP, and C4-2 were treated with CFI-400945, stained with propidium iodide, and analyzed by flow cytometry. The data were analyzed using one-way ANOVA followed by Dunnett's multiple comparison tests and presented as means  $\pm$  SEM with statistical significance (\*\* $p < 0.01$ ; \*\*\* $p < 0.001$ ) for G2/M cell cycle arrest. (F) HPrEC and PCa cell lines were treated with CFI-400945 and stained for  $\beta$ -galactosidase. The representative images at 40x magnification from each treatment group are presented. (G) SA- $\beta$ -Gal-positive cells were scored in four different fields. Results are expressed as the mean percentage of SA- $\beta$ -Gal-positive cells (mean  $\pm$  SEM). (H,I) CDKN1A (p21) mRNA and protein levels in PCa cells. GAPDH was used as an endogenous control for CDKN1A mRNA analysis. Vinculin was used as a protein loading control. The data represent three biological replicates. ANOVA, analysis of variance; CA, centrosome amplification; DMSO, dimethyl sulfoxide; HPrEC, human primary prostate epithelial cell; mRNA, messenger RNA; PCa, prostate cancer; PLK4, polo-like kinase 4; SA- $\beta$ -Gal, senescence-associated  $\beta$ -galactosidase. [Color figure can be viewed at [wileyonlinelibrary.com](http://wileyonlinelibrary.com)]

including anticancer drugs, and is often associated with elevated reactive oxygen species, cell cycle regulators (e.g., p21), and senescence-associated secretory phenotype (SASP), which includes immunostimulatory cytokines, chemokines to recruit lymphocytes, and metalloproteinases.<sup>46</sup> However, SASP can also be immunosuppressive, as has been associated with immunosuppressive cytokines such as TGF- $\beta$ . It will be interesting to further study how PLK4 inhibitors cause senescence in vivo, if this is associated with pro- or anti-inflammatory phenotypes, and whether PLK4 inhibitors may synergize with immune checkpoint blockade in treating cancer.

Our data address several important questions regarding CA in PCa. The relative contributions of two major mechanisms leading to CA (centriole overduplication vs. doubling events) were unclear before this investigation. We have shown that most CA is due to centriole overduplication rather than doubling events in PCa. Indeed, additional studies to determine the drivers of centriole duplication in cancer are warranted. In vitro experimental evidence has suggested that overexpression of PLK4,<sup>18</sup> SAS6,<sup>47</sup> STIL,<sup>48</sup> and pericentrin<sup>49</sup> and loss of MCPH1,<sup>50</sup> among others, can result in centriole overduplication. However, the actual causes of CA in human cancers have not been fully elucidated.

There are some limitations to our analysis. First, we may be underestimating CA in PCa because we look at PCM markers (pericentrin and  $\gamma$ -tubulin) but not centriole markers (e.g., centrin) in primary PCa specimens. Sometimes extra centrioles can be masked by one large PCM focus. Second, we have used mother centriole markers to distinguish centriole overduplication from cell doubling. If cells with centriole overduplication progressed through late G2 when CEP164 is recruited to nascent mature centriole,<sup>24</sup> we would underestimate CA due to centriole overduplication and overestimate CA due to doubling events. However, we actually observed a decrease in the percentage of centrosomes containing CEP164 in PCa compared to benign controls, suggesting that this did not substantially impact our analysis. Additionally, the visualization of centrosomes may be impacted by sectioning artifacts in the underestimation of CA. Similarly, overestimated CA count cannot be ruled out, as not every pericentrin focus may represent a real centrosome with centrioles.

Overall, our study suggests a proliferative role of PLK4 in PCa warranting future investigation into targeting PLK4 for PCa management. Further studies will be needed to identify relevant biomarkers associated with sensitivity and clinical response to PLK4 inhibitors, which could not only improve patient selection and provide a means to monitor treatment efficacy but also open door to new therapeutic combination strategies.

#### AUTHOR CONTRIBUTIONS

Chandra K. Singh, Ryan A. Denu, and Nihal Ahmad drafted the study. Chandra K. Singh, Ryan A. Denu, Minakshi Nihal, Maria Shabbir and Debra R. Garvey performed the experiments. Chandra K. Singh, Ryan A. Denu, and Wei Huang analyzed the data. Kenneth A. Iczkowski

provided TMA and clinical data. Chandra K. Singh and Ryan A. Denu wrote the manuscript. Nihal Ahmad supervised the study. All authors critically reviewed, revised, and approved the manuscript.

#### ACKNOWLEDGMENTS

The authors thank Dr. Erich Nigg and Elena Nigg for reagents; the University of Wisconsin Translational Research Initiatives in Pathology laboratory (TRIP) for use of its facilities and services; and the University of Wisconsin Carbone Cancer Center's Experimental Animal Pathology and Flow cytometry labs. The research reported in this publication was supported by the National Institutes of Health under the following awards: F30CA203271, T32GM008692, P30 CA014520, R01CA176748, and S10OD023526. This study was also supported by the Department of Veterans Affairs (VA Merit Review Awards I01CX001441 and I101BX004221, and a Research Career Scientist Award IK6BX003780 to Nihal Ahmad). The content is the responsibility of the authors and does not necessarily represent the views of the NIH or VA.

#### CONFLICTS OF INTEREST

The authors declare no conflicts of interest.

#### DATA AVAILABILITY STATEMENT

The data that supports the findings of this study are available in the manuscript and Supplementary Materials of this article.

#### ORCID

Chandra K. Singh  <http://orcid.org/0000-0003-3505-0350>

Kenneth A. Iczkowski  <http://orcid.org/0000-0003-1370-6435>

Nihal Ahmad  <http://orcid.org/0000-0002-4239-9887>

#### REFERENCES

- Denu RA, Zasadil LM, Kanugh C, Laffin J, Weaver BA, Burkard ME. Centrosome amplification induces high grade features and is prognostic of worse outcomes in breast cancer. *BMC Cancer*. 2016;16(1):47.
- Siegel RL, Miller KD, Fuchs HE, Jemal A. Cancer statistics, 2021. *CA Cancer J Clin*. 2021;71(1):7-33.
- Pihan GA, Purohit A, Wallace J, et al. Centrosome defects and genetic instability in malignant tumors. *Cancer Res*. 1998;58(17):3974-3985.
- Pihan GA, Purohit A, Wallace J, Malhotra R, Liotta L, Doxsey SJ. Centrosome defects can account for cellular and genetic changes that characterize prostate cancer progression. *Cancer Res*. 2001;61(5):2212-2219.
- Toma MI, Friedrich K, Meyer W, et al. Correlation of centrosomal aberrations with cell differentiation and DNA ploidy in prostate cancer. *Anal Quant Cytol Histol*. 2010;32(1):1-10.
- Pihan GA, Wallace J, Zhou Y, Doxsey SJ. Centrosome abnormalities and chromosome instability occur together in pre-invasive carcinomas. *Cancer Res*. 2003;63(6):1398-1404.
- Godinho SA, Pellman D. Causes and consequences of centrosome abnormalities in cancer. *Philos Trans R Soc Lond B*. 2014;369(1650).
- Denu RA, Shabbir M, Nihal M, et al. Centriole overduplication is the predominant mechanism leading to centrosome amplification in melanoma. *Mol Cancer Res*. 2018;16(3):517-527.



9. Glover DM, Hagan IM, Tavares AA. Polo-like kinases: a team that plays throughout mitosis. *Genes Dev.* 1998;12(24):3777-3787.
10. Swallow CJ, Ko MA, Siddiqui NU, Hudson JW, Dennis JW. Sak/Plk4 and mitotic fidelity. *Oncogene.* 2005;24(2):306-312.
11. Macmillan JC, Hudson JW, Bull S, Dennis JW, Swallow CJ. Comparative expression of the mitotic regulators SAK and PLK in colorectal cancer. *Ann Surg Oncol.* 2001;8(9):729-740.
12. Marina M, Saavedra HI. Nek2 and Plk4: prognostic markers, drivers of breast tumorigenesis and drug resistance. *Front Biosci.* 2014;19:352-365.
13. Li Z, Dai K, Wang C, et al. Expression of polo-like kinase 4(PLK4) in breast cancer and its response to taxane-based neoadjuvant chemotherapy. *J Cancer.* 2016;7(9):1125-1132.
14. Tian X, Zhou D, Chen L, et al. Polo-like kinase 4 mediates epithelial-mesenchymal transition in neuroblastoma via PI3K/Akt signaling pathway. *Cell Death Dis.* 2018;9(2):54.
15. Ko MA, Rosario CO, Hudson JW, et al. Plk4 haploinsufficiency causes mitotic infidelity and carcinogenesis. *Nat Genet.* 2005;37(8):883-888.
16. Levine MS, Bakker B, Boeckx B, et al. Centrosome amplification is sufficient to promote spontaneous tumorigenesis in mammals. *Dev Cell.* 2017;40(3):313-322.e315.
17. Serçin Ö, Larsimont JC, Karambelas AE, et al. Transient PLK4 overexpression accelerates tumorigenesis in p53-deficient epidermis. *Nat Cell Biol.* 2016;18(1):100-110.
18. Godinho SA, Picone R, Burute M, et al. Oncogene-like induction of cellular invasion from centrosome amplification. *Nature.* 2014;510(7503):167-171.
19. Kazazian K, Go C, Wu H, et al. Plk4 promotes cancer invasion and metastasis through Arp2/3 complex regulation of the actin cytoskeleton. *Cancer Res.* 2017;77(2):434-447.
20. Pannu V, Mittal K, Cantuaria G, et al. Rampant centrosome amplification underlies more aggressive disease course of triple negative breast cancers. *Oncotarget.* 2015;6(12):10487-10497.
21. Rosario CO, Kazazian K, Zih FS, et al. A novel role for Plk4 in regulating cell spreading and motility. *Oncogene.* 2015;34(26):3441-3451.
22. Korzeniewski N, Hohenfellner M, Duensing S. CAND1 promotes PLK4-mediated centriole overduplication and is frequently disrupted in prostate cancer. *Neoplasia.* 2012;14(9):799-806.
23. Mittal K, Kaur J, Sharma S, et al. Hypoxia drives centrosome amplification in cancer cells via HIF1alpha-dependent induction of polo-like kinase 4. *Mol Cancer Res.* 2022.
24. Graser S, Stierhof YD, Lavoie SB, et al. Cep164, a novel centriole appendage protein required for primary cilium formation. *J Cell Biol.* 2007;179(2):321-330.
25. Garcia-Peterson LM, Ndiaye MA, Singh CK, Chhabra G, Huang W, Ahmad N. SIRT6 histone deacetylase functions as a potential oncogene in human melanoma. *Genes Cancer.* 2017;8(9-10):701-712.
26. Wang X, Spandidos A, Wang H, Seed B. PrimerBank: a PCR primer database for quantitative gene expression analysis, 2012 update. *Nucleic Acids Res.* 2012;40(Database issue):D1144-D1149.
27. George J, Nihal M, Singh CK, Ahmad N. 4'-Bromo-resveratrol, a dual Sirtuin-1 and Sirtuin-3 inhibitor, inhibits melanoma cell growth through mitochondrial metabolic reprogramming. *Mol Carcinog.* 2019;58(10):1876-1885.
28. Franken NA, Rodermond HM, Stap J, Haveman J, van Bree C. Clonogenic assay of cells in vitro. *Nat Protoc.* 2006;1(5):2315-2319.
29. Guarguaglini G, Duncan PI, Stierhof YD, Holmstrom T, Duensing S, Nigg EA. The forkhead-associated domain protein Cep170 interacts with Polo-like kinase 1 and serves as a marker for mature centrioles. *Mol Biol Cell.* 2005;16(3):1095-1107.
30. Duensing A, Ghanem L, Steinman RA, Liu Y, Duensing S. p21(Waf1/Cip1) deficiency stimulates centriole overduplication. *Cell Cycle.* 2006;5(24):2899-2902.
31. Press MF, Xie B, Davenport S, et al. Role for polo-like kinase 4 in mediation of cytokinesis. *Proc Natl Acad Sci USA.* 2019;116(23):11309-11318.
32. Singh CK, Malas KM, Tydrick C, Siddiqui IA, Iczkowski KA, Ahmad N. Analysis of zinc-exporters expression in prostate cancer. *Sci Rep.* 2016;6:36772.
33. Ogden A, Rida PC, Aneja R. Prognostic value of CA20, a score based on centrosome amplification-associated genes, in breast tumors. *Sci Rep.* 2017;7(1):262.
34. Gao J, Aksoy BA, Dogrusoz U, et al. Integrative analysis of complex cancer genomics and clinical profiles using the cBioPortal. *Sci Signal.* 2013;6(269):pl1.
35. Mason JM, Lin DC, Wei X, et al. Functional characterization of CFI-400945, a Polo-like kinase 4 inhibitor, as a potential anticancer agent. *Cancer Cell.* 2014;26(2):163-176.
36. Sampson PB, Liu Y, Forrest B, et al. The discovery of Polo-like kinase 4 inhibitors: identification of (1R,2S)-2-(3-((E)-4-(((cis)-2,6-dimethylmorpholino)methyl)styryl)-1H-indazol-6-yl)-5'-methoxyspiro[cyclopropane-1,3'-indolin]-2'-one (CFI-400945) as a potent, orally active antitumor agent. *J Med Chem.* 2015;58(1):147-169.
37. Wong YL, Anzola JV, Davis RL, et al. Cell biology. Reversible centriole depletion with an inhibitor of Polo-like kinase 4. *Science.* 2015;348(6239):1155-1160.
38. Hudson JW, Kozarova A, Cheung P, et al. Late mitotic failure in mice lacking Sak, a polo-like kinase. *Curr Biol.* 2001;11(6):441-446.
39. Dinçer T, Yorgancıoğlu-Budak G, Ölmez A, et al. Analysis of centrosome and DNA damage response in PLK4 associated Seckel syndrome. *Eur J Hum Genet.* 2017;25(10):1118-1125.
40. Holland AJ, Fachinetti D, Da Cruz S, et al. Polo-like kinase 4 controls centriole duplication but does not directly regulate cytokinesis. *Mol Biol Cell.* 2012;23(10):1838-1845.
41. Sir JH, Pütz M, Daly O, et al. Loss of centrioles causes chromosomal instability in vertebrate somatic cells. *J Cell Biol.* 2013;203(5):747-756.
42. Denu RA, Sass MM, Johnson JM, et al. Polo-like kinase 4 maintains centriolar satellite integrity by phosphorylation of centrosomal protein 131 (CEP131). *J Biol Chem.* 2019;294(16):6531-6549.
43. Meitinger F, Anzola JV, Kaulich M, et al. 53BP1 and USP28 mediate p53 activation and G1 arrest after centrosome loss or extended mitotic duration. *J Cell Biol.* 2016;214(2):155-166.
44. Lambrus BG, Daggubati V, Uetake Y, et al. A USP28-53BP1-p53-p21 signaling axis arrests growth after centrosome loss or prolonged mitosis. *J Cell Biol.* 2016;214(2):143-153.
45. Fong CS, Mazo G, Das T, et al. 53BP1 and USP28 mediate p53-dependent cell cycle arrest in response to centrosome loss and prolonged mitosis. *eLife.* 2016;5:e16270.
46. Prieto LI, Baker DJ. Cellular senescence and the immune system in cancer. *Gerontology.* 2019;65(5):505-512.
47. Shinmura K, Kato H, Kawanishi Y, et al. SASS6 overexpression is associated with mitotic chromosomal abnormalities and a poor prognosis in patients with colorectal cancer. *Oncol Rep.* 2015;34(2):727-738.
48. Tang CJ, Lin SY, Hsu WB, et al. The human microcephaly protein STIL interacts with CPAP and is required for procentriole formation. *EMBO J.* 2011;30(23):4790-4804.
49. Loncarek J, Hergert P, Magidson V, Khodjakov A. Control of daughter centriole formation by the pericentriolar material. *Nat Cell Biol.* 2008;10(3):322-328.



50. Denu RA, Burkard ME. Analysis of the "centrosome-ome" identifies MCPH1 deletion as a cause of centrosome amplification in human cancer. *Sci Rep*. 2020;10(1):11921.

#### **SUPPORTING INFORMATION**

Additional supporting information may be found in the online version of the article at the publisher's website.

**How to cite this article:** Singh CK, Denu RA, Nihal M, et al. PLK4 is upregulated in prostate cancer and its inhibition reduces centrosome amplification and causes senescence. *The Prostate*. 2022;82:957-969. doi:10.1002/pros.24342